

Adaptive t -Design Dummy-Gate Obfuscation for Cryogenic-Scale Enforcement

Samuel Punch
School of Computer Science
University College Cork
Cork, Ireland
samuel.punch@ucc.ie

Krishnendu Guha
School of Computer Science
University College Cork
Cork, Ireland
k.guha@ucc.ie

Abstract—Cloud quantum services can reveal circuit structure and timing via scheduler metadata, latency patterns, and co-tenant interference. We introduce *NADGO* (Noise-Adaptive Dummy-Gate Obfuscation), a scheduling & obfuscation stack that enforces *operational privacy* for gate-model workloads by applying per-interval limits on observable information leakage. To support confidentiality and fair multi-tenancy, operators need a way to *audit* compliance at acceptable overheads. *NADGO* combines: (i) hardware-aware t -design padding for structured cover traffic; (ii) particle-filter timing randomisation to mask queue patterns; (iii) CASQUE subcircuit routing across heterogeneous backends; and (iv) a per-interval leakage estimator $\hat{\Delta}_t$ with locked calibration artefacts and a dual-threshold kill-switch. We prototype on a 4-qubit superconducting tile with cryo-CMOS control and evaluate depth-varied local-random circuits and small QAOA instances. Monitoring runs at a $6.3\mu\text{s}$ control interval, and we record per-interval decisions in an append-only, hash-chained audit log. Across Monte Carlo (Tier I) and cloud-hardware emulation (Tier II) evaluations, *NADGO* keeps $\hat{\Delta}_t \leq \Delta_{\text{budget}}$ in nominal operation (interval-abort SLO $\leq 1\%$) and, under attack, yields high AUC separation with concentrated aborts. At matched leakage targets, microbenchmarks indicate lower latency and cryogenic power than static padding, while end-to-end workloads maintain competitive cost envelopes.

I. INTRODUCTION

Multi-tenant quantum clouds expose *operational* side channels such as queue timing, scheduler metadata, and co-tenant crosstalk that can reveal circuit structure even when outputs are correct [1]–[3]. Such leakage threatens confidentiality and fair multi-tenancy, and persists despite correctness/verification guarantees that focus on outputs rather than operations [1].

Challenges. Deployable defences must: (i) operate at run time on μs -scale control loops, (ii) adapt to device drift and heterogeneous back ends, (iii) quantify leakage from operational traces, (iv) support *abort* semantics with auditable logs, and (v) respect latency/power budgets.

Prior work and limitations. Static padding and fixed-rate batching regularise timing but ignore drift and workload variation; reported mitigations typically act in isolation from compilation, routing, and run-time enforcement [2]. Correctness and verifiability protocols protect outputs (and, in blind protocols, algorithm content) rather than the emitted operational metadata [1]. State and unitary t -designs hide state structure but are rarely integrated with schedulers/routers and lack per-interval enforcement [4]–[6]. Noise- and calibration-aware

compilation improves fidelity under drift yet does not address timing/metadata side channels [7], [8]. Interface- and scheduler-level studies further evidence practical leaks in today’s stacks [2], [3].

Motivating example. A tenant submits circuits of two depths, $D_1 < D_2$. An insider observing queue and latency patterns can infer depth via clustering. Our monitor estimates $\hat{\Delta}_t$ from observable features; if $\hat{\Delta}_t \geq \Delta_{\text{kill}}$, execution aborts and the event is immutably logged. In §VI we show reduced timing correlation versus baselines under the same policy.

Our work (NADGO). *NADGO* (Noise-Adaptive Dummy-Gate Obfuscation) enforces per-interval leakage limits via: hardware-aware t -design padding, drift-adaptive timing randomisation, CASQUE sub-circuit routing, and a locked policy $(\Delta_{\text{budget}}, \Delta_{\text{kill}})$ with an automatic kill-switch and audit.

Contributions.

- **Metric & policy.** An instantaneous estimator $\hat{\Delta}_t$ for Δ_t with a per-interval policy $(\Delta_{\text{budget}}, \Delta_{\text{kill}})$ that composes across layers (§IV; Thm. V.1).
- **Orchestration.** The *NADGO*+CASQUE pipeline combining t -design padding, particle-filter timing randomisation, CASQUE sub-circuit routing, and a monitored kill-switch; the per-job procedure is given in Algorithm 2.
- **Evaluation.** A 4-qubit cryo-CMOS prototype with a $6.3\mu\text{s}$ control interval; we report end-to-end overheads and leakage control versus baselines under identical policies (Section VI).

This article is organised as follows. Section II reviews operational leakage and related work. Section III states the system and threat model. Section IV details the estimator, padding, timing, routing, and orchestration. Section VI reports empirical results, with Section VII discussing limitations and outlook.

II. BACKGROUND AND RELATED WORK

Operational leakage and side-channels. Multi-tenant control planes leak via timing traces, scheduler metadata, and co-tenant interference—signals that persist even when outputs are correct [1]. On superconducting stacks, bias-current fluctuations in SFQ–DC converters and SQUID arrays yield distinctive profiles that reveal control events [3]. At the orchestration layer, Lu *et al.* show current clouds expose circuit structure

through pulse cadence, calibration events, and job descriptors; proposed fixes (e.g., randomised scheduling) act in isolation from compilation, routing, and run-time enforcement [2]. These realities motivate NADGO’s unified defence— t -design padding, drift-adaptive timing, topology-aware routing, and *per-interval* policy enforcement; a structured comparison appears in Table I.

Leakage metric and run-time policies. We use an instantaneous leakage metric ΔI_t with a per-interval policy ($\Delta_{\text{budget}}, \Delta_{\text{kill}}$) to prevent burst leakage being hidden by averages. Following Mardia *et al.* [9], sharp concentration bounds for empirical discrete distributions improve reliability over short windows, enabling low false-positive kill-switch triggers while retaining burst sensitivity.

t -design padding and timing randomisation. State t -designs— ϵ -approximate ensembles matching the first t Haar moments—provably hide state structure from polynomial-time adversaries [4]. Ambainis–Emerson show $t \geq 4$ designs are indistinguishable from Haar-random states; Haferkamp *et al.* [6] give tighter depth bounds, and Brandão–Harrow–Horodecki [5] extend to local random circuits. NADGO uses hardware-aware, $t \geq 4$ padding with native-gate constraints to fit coherence budgets, integrating timing perturbations to obfuscate execution cadence, which was not the focus of prior works.

Calibration-aware compilation and drift mitigation. Noise non-stationarity limits “latest-only” calibration snapshots. Kurniawan *et al.* [7] show historical windows improve fidelity; Ferrari–Amoretti [8] adapt compilation to heavy-hex layouts. NADGO extends these noise-aware features to operational privacy, feeding calibration trends into a drift-aware scheduler for topology- and timing-randomised routing.

Noise-adaptive co-search. QuantumNAS [10] couples circuit topology search with qubit mapping for noise robustness. In NADGO, similar noise-awareness also informs dummy padding and timing randomisation for joint fidelity/privacy optimisation.

Cryogenic hardware characterisation and control. Cryo-CMOS control electronics at mK–few-K temperatures require accurate modelling. Pérez-Bailón *et al.* [11] and Eastoe *et al.* [12] provide measurement and modelling techniques informing NADGO’s latency budgets and leakage/noise models for sub-10 μs enforcement.

Phase-based obfuscation for compiler threats. OPAQUE [13] hides keys in R_Z rotation angles for IP protection, but does not address timing or metadata leakage; it is complementary to NADGO.

Scope and comparison. Table I summarises representative approaches against the four challenges we target (run-time overhead management, drift adaptation, topology awareness, and operational privacy), and situates NADGO alongside prior work.

Positioning. NADGO targets operational privacy for gate-model quantum clouds, integrating t -design padding, drift-adaptive timing, topology-aware routing, and auditable kill-switch monitoring. Unlike prior art, which addresses only subsets of Table I, the proposed framework of NADGO addresses and unifies all four under dynamic, multi-tenant conditions.

TABLE I
REPRESENTATIVE APPROACHES VS. KEY CHALLENGES (Y = ADDRESSED; – = NOT IN SCOPE).

Framework	RT Overhd	Drift Adapt.	Topo. Aware	OP Priv.	Scale
Scheduler leakage [2]	–	–	–	Y	cloud
State t -designs (A&E’07) [4]	–	–	–	Y	theory
Calib.-aware [7]	–	Y	–	–	7–127 q
Noise-adapt. comp. [8]	–	Y	Y	–	SC (bench)
Cryo-CMOS (scale) [12]	Y	–	Y	–	large
OPAQUE [13]	–	–	–	Y	20–50 q
This work: NADGO	Y	Y	Y	Y	4–32 q (proto)

Run-time overhead: actively manages latency/effort; *Drift adaptivity:* adapts to time-varying noise; *Topology awareness:* placement/routing respects hardware; *Operational privacy:* timing/metadata protections.

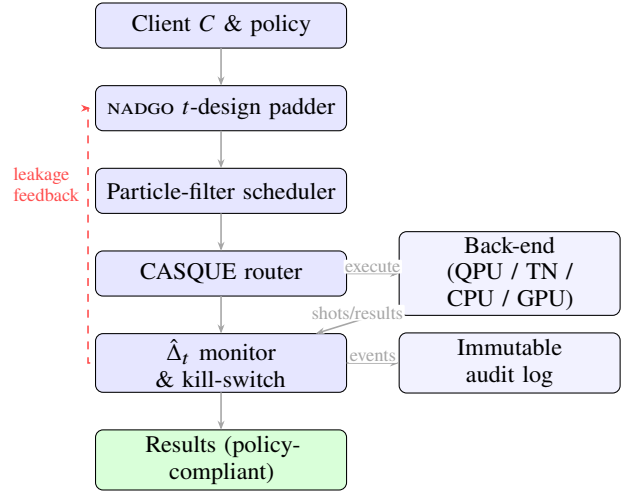


Fig. 1. Vertical system pipeline: policy-aligned compilation, secure padding, adaptive scheduling/routing, and monitored execution with leakage-bound enforcement and audit logging.

III. SYSTEM AND THREAT MODEL

We enforce a per-interval leakage policy ($\Delta_{\text{budget}}, \Delta_{\text{kill}}$) with a quantum–classical pipeline that adapts to hardware drift and aborts if estimated leakage exceeds policy limits. The pipeline has four stages—policy-aligned compilation, secure padding, adaptive scheduling/routing, and monitored execution with audit—with feedback to retune padding on-line (Fig. 1). The threat model (Fig. 2) maps adversaries and attack surfaces to the mitigations evaluated in our experiments.

System Overview

Client-side compilation (*Qiskit/tket*) produces policy-aligned circuits. The NADGO t -design padder injects dummy gates to provide cover traffic. A particle-filter scheduler adapts dispatch under drift; CASQUE routing spreads segments across a heterogeneous back-end. The $\hat{\Delta}_t$ monitor enforces thresholds in real time, aborting on violations and appending to a write-once audit log. Leakage feedback tunes padding parameters.

Threat Model

Our goal is to maintain $\hat{\Delta}_t \leq \Delta_{\text{budget}}$ during nominal operation, abort when $\hat{\Delta}_t \geq \Delta_{\text{kill}}$, and record verifiable audit

**Tier I scope ($n \in \{4, 8, 16\}$):
evaluated $A \rightarrow T \rightarrow M$ mappings**

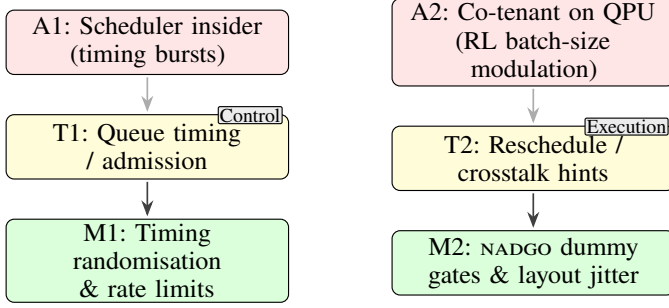


Fig. 2. Threat model (evaluated scope): two parallel chains, $A1 \rightarrow T1 \rightarrow M1$ (Control) and $A2 \rightarrow T2 \rightarrow M2$ (Execution).

events. Adversaries can observe control-plane timing, scheduling behaviour, and coarse telemetry, but cannot compromise the policy engine or perform invasive hardware attacks.

Adversaries and evaluated mitigations.: We consider two evaluated classes (A1–A2) mapped to attack surfaces (T1–T2) and mitigations (M1–M2). Tier I evaluates $A1 \rightarrow T1$ and $A2 \rightarrow T2$; telemetry-side channels are out of experimental scope.

IV. METHODOLOGY

We formalise the leakage-control objective, specify each NADGO layer (padding, timing, routing, monitoring), and give an operational-privacy (OP-IND) bound. Calibration choices are fixed and auditable to enable reproducibility.

A. Leakage Objective and Estimator

Let U_{real} be the hidden computation, U_{obs} observable traces (timing/metadata/telemetry), Λ_C the crosstalk channel, and Y public side information. We measure instantaneous leakage as

$$\Delta I_t \triangleq \sup_{A \in \mathcal{A}_{\text{poly}}} I(U_{\text{real}}; A(U_{\text{obs}}) | \Lambda_C, Y), \quad (1)$$

and enforce a dual-threshold policy ($\Delta_{\text{budget}}, \Delta_{\text{kill}}$): continue if $\Delta I_t \leq \Delta_{\text{budget}}$, abort if $\Delta I_t \geq \Delta_{\text{kill}}$.

a) Estimator.: We estimate ΔI_t via a divergence to a locked t -design reference with a crosstalk penalty:

$$\widehat{\Delta}_t = \min \left\{ D_{\text{KL}}(\widehat{p}_t \| p_t^{(\text{des})}) + \beta_{\text{est}} \|\Lambda_C\|_F, \Delta_{\text{kill}} \right\}, \quad (2)$$

where $p_t^{(\text{des})}$ is the design-only reference (per job size and segment class), \widehat{p}_t is the empirical cadence distribution, and β_{est} is a fixed weight.

b) Cadence features and assumptions.: We extract a compact feature alphabet \mathcal{S} each interval: inter-dispatch gap Δt , batch-size ratio b (normalised to a design baseline), queue state q (categorical), and a scalar telemetry proxy ζ . We assume (A1) feature sufficiency for U_{obs} ; (A2) Lipschitz crosstalk impact; (A3) conditional independence across intervals given (Λ_C, Y) .

c) Calibration (windowing, quantisation, smoothing; locked across tiers).: To make (2) reproducible, we fix the following pipeline:

- *Windowing*: sliding-window length $W=128$ intervals; stride $S=64$ (half overlap). We form a window histogram over codewords and apply an EMA with half-life $H=10$ windows.
- *Normalisation*: $\widehat{\Delta t} = \Delta t / \mu_{\Delta t}(n)$, $\widehat{b} = b / \mu_b(n)$ using design-only baselines for job size n .
- *Vector quantisation (fixed codebook)*: bins per feature

$B_{\Delta t} = 16$ (design quantiles),

$B_b = 5 \{ \leq 0.5, (0.5, 0.9], (0.9, 1.1], (1.1, 1.5], > 1.5 \}$,

$B_q = 4$ (idle, light, moderate, heavy),

$B_\zeta = 8$ (design quantiles).

This yields $B = 16 \times 5 \times 4 \times 8 = 2560$ codewords. The mapping from $(\Delta t, b, q, \zeta)$ to an index $c_u \in \{1, \dots, B\}$ is fixed at calibration.

- *Smoothing*: Jeffreys add- α with $\alpha = \frac{1}{2}$ for both reference and empirical histograms; an EMA combines successive windows. We also mix a tiny uniform mass $\lambda = 10^{-3}$ into the design reference to guarantee strict positivity.
- *Locked reference*: for each $(n, \text{segment})$ class we collect $M \approx 10^6$ design-only intervals to build $p_{n,k}^{(\text{des})}$; we persist $\{p_{n,k}^{(\text{des})}\}$, bin edges, and $(W, S, H, \alpha, \lambda)$ with a checksum. Online, we select $p_t^{(\text{des})}$ by (n, k) and compute \widehat{p}_t with the same codebook.

Lemma IV.1 (Estimator upper bound). *Under (A1)–(A3) and mild regularity of Λ_C ,*

$$\sup_{A \in \mathcal{A}_{\text{poly}}} I(U_{\text{real}}; A(S_t) | \Lambda_C, Y) \leq D_{\text{KL}}(\widehat{p}_t \| p_t^{(\text{des})}) + \beta_{\text{est}} \|\Lambda_C\|_F.$$

B. Noise-Adaptive t -Design Padding

We insert ε_{des} -approximate t -design layers ($t = \lceil \log_2 n \rceil$, $\varepsilon_{\text{des}} = 0.02$) using native Clifford scaffolds. Depth is $O(n \log n)$ with hardware-aware templates to minimise compilation overhead. The padding both randomises observable cadence and aligns window statistics with $p^{(\text{des})}$.

C. Particle-Filter Timing Randomisation

Padding alone cannot hide queue cadence. We therefore jitter dispatch times θ_k using a queue-aware particle filter:

$$\theta_k \sim \text{PF}(\theta_{k-1}; \sigma_t, \ell_{\text{max}}, q_k), \quad \eta^{(i)} \sim \mathcal{N}(0, \sigma_{\text{proc}}^2(q_k)),$$

with proposals $\theta_k^{(i)} \leftarrow \text{clamp}(\theta_{k-1}^{(i)} + \eta^{(i)}, \pm \sigma_t)$ and weights set to 0/1 by an ℓ_{max} latency constraint. We trigger resampling when the effective sample size $\text{ESS} < N/2$. The jitter variance $\sigma_{\text{proc}}(\cdot)$ widens with backlog q_k .

D. CASQUE Sub-Circuit Routing

Given padded segments $\{C'_k\}$, we select a backend h by minimising a multi-objective cost

$$\text{Cost}(h) = \alpha(1 - \widehat{\text{Fid}}(h)) + \omega_{\text{leak}} \text{LeakRisk}(h) + \gamma \text{QueuePenalty}(h). \quad (3)$$

Algorithm 1: PF-TimingSampler (queue-aware jitter control)

Input: Particles $\{\theta_{k-1}^{(i)}, w_{k-1}^{(i)}\}_{i=1}^N$; base jitter σ_t ; max-latency ℓ_{\max} ; queue state q_k
Output: Updated particles $\{\theta_k^{(i)}, w_k^{(i)}\}_{i=1}^N$
for $i=1$ **to** N **do**
 $\eta^{(i)} \sim \mathcal{N}(0, \sigma_{\text{proc}}^2(q_k))$;
 $\theta_k^{(i)} \leftarrow \text{clamp}(\theta_{k-1}^{(i)} + \eta^{(i)}, \pm\sigma_t)$;
 $w_k^{(i)} \leftarrow w_{k-1}^{(i)} \cdot \mathbf{1}[\text{LATENCY}(\theta_k^{(i)}, q_k) \leq \ell_{\max}]$;
Normalise weights;
if $\text{ESS} < N/2$ **then**
 Resample and set $w_k^{(i)} \leftarrow 1/N$

Algorithm 2: NADGO Orchestration (per job)

Input: Circuit C ; locked artefacts $(q_{\text{ref}}, p^{(\text{des})}, \text{codebook})$; thresholds $(\Delta_{\text{budget}}, \Delta_{\text{kill}})$
Output: Results or abort; append-only audit log
 $C' \leftarrow \text{INSERTTDESIGN}(C)$; Segment $C' \rightarrow \{C'_k\}_{k=1}^K$;
for $k=1$ **to** K **do**
 $\theta_k \leftarrow \text{PF_PROPOSE}(q_k)$ // Alg. 1
 $h_k \leftarrow \text{SELECTBACKEND}(C'_k)$ // CASQUE cost minimisation
 $\text{EXECUTE}(C'_k, h_k, \theta_k)$; $\hat{\Delta}_t \leftarrow \text{UPDATEESTIMATOR}()$;
 $\text{LOG}(k, h_k, \theta_k, \hat{\Delta}_t)$;
 if $\hat{\Delta}_t \geq \Delta_{\text{kill}}$ **then**
 ABORTANDATTEST(); **return**
FUSERESULTS(); FINALIZELOG(); **return**

where $\widehat{\text{Fid}}$ is a hardware-calibrated fidelity proxy, LeakRisk uses $\hat{\Delta}_t$ as a signal, and QueuePenalty scores tail pressure. We switch if $\hat{\Delta}_t \geq \Delta_{\text{budget}} - \tau$ for m consecutive intervals or when a candidate yields a relative cost drop $\geq \delta$. (Weights $\alpha, \omega_{\text{leak}}, \gamma$ and hysteresis (τ, m, δ) are fixed across experiments.)

E. Monitoring, Kill-Switch, and Audit

A lightweight monitor updates $\hat{\Delta}_t$ each interval and issues an abort if $\hat{\Delta}_t \geq \Delta_{\text{kill}}$, completing in $< 5 \mu\text{s}$. All decisions (segment, backend, jitter, thresholds, $\hat{\Delta}_t$) are hashed into an append-only audit log.

F. Orchestration (Per-Job)

Algorithm 2 summarises the per-job control flow and its calls to PF timing (Alg. 1).

G. Operational-Privacy Game and Bound

a) OP-IND (pointer).: We adopt the OP-IND game defined above; the privacy bound is stated in Theorem V.1 (Sec. V).

b) Notes on reproducibility.: All estimator hyperparameters $(W, S, H, \alpha, \lambda, B)$, codebook edges, and $\{p_{n,k}^{(\text{des})}\}$ are persisted with a checksum and reused unchanged across tiers. Routing/monitoring hyperparameters $(\alpha, \omega_{\text{leak}}, \gamma, \tau, m, \delta)$ are fixed once and remain unchanged across experiments.

V. SECURITY ARGUMENT

We assess *operational privacy* via the OP-IND game: the adversary chooses C_0, C_1 with $\text{pub}(C_0) = \text{pub}(C_1)$; orchestration (Sec. III) runs under $(\Delta_{\text{budget}}, \Delta_{\text{kill}})$ and reveals the transcript τ (timing/metadata and abort flag). Let $\hat{\Delta}_t$ denote the estimator from Sec. IV, and let \mathcal{T} be the set of admitted (non-aborting) intervals.

Theorem V.1 (OP-IND advantage). *Assume $\hat{\Delta}_t \leq \Delta_{\text{budget}}(t)$ for all $t \in \mathcal{T}$, calibration $|\mathbb{E}[\hat{\Delta}_t] - \Delta_t| \leq \epsilon_{\text{est}}(t)$, and bounded skew/jitter ϵ_{sync} . Then for any PPT adversary,*

$$\text{Adv}_{\mathcal{A}}^{\text{OP-IND}}(\mathcal{T}) \leq \sum_{t \in \mathcal{T}} \sqrt{2 \Delta_{\text{budget}}(t)} + \sum_{t \in \mathcal{T}} \sqrt{2} (\epsilon_{\text{est}}(t) + \epsilon_{\text{sync}}). \quad (4)$$

Corollary V.1 (Uniform budgets). *If $\Delta_{\text{budget}}(t) = \Delta_{\text{budget}}$ and $\epsilon_{\text{est}}(t) \leq \bar{\epsilon}_{\text{est}}$ for all $t \in \mathcal{T}$ with $|\mathcal{T}| = T$, then*

$$\text{Adv}_{\mathcal{A}}^{\text{OP-IND}} \leq T \sqrt{2 \Delta_{\text{budget}}} + T \sqrt{2} (\bar{\epsilon}_{\text{est}} + \epsilon_{\text{sync}}),$$

i.e., advantage scales linearly in T and as $\sqrt{\Delta_{\text{budget}}}$ per interval.

Proof idea. Pinsker bounds per-interval total variation via KL; the policy upper-bounds KL through $\hat{\Delta}_t$. A hybrid over admitted intervals gives (4); aborts simply shorten \mathcal{T} .

VI. EXPERIMENTAL EVALUATION

a) Metrics.: Unless stated otherwise, latency and power are reported *per admitted interval* (conditional on non-abort); per-episode summaries appear only when explicitly labelled.

b) Thresholds (reporting & rationale).: Exact $(\Delta_{\text{budget}}, \Delta_{\text{kill}})$ used in each run are recorded in the experimentation code (versioned configs and per-run logs). We set thresholds *per experiment* (e.g., by job size n , workload, environment) by targeting baseline quantiles of $\hat{\Delta}_t$ with a small hysteresis gap, fixing a nominal false-alarm rate and stabilising decisions under distributional shift. For Tier II, the Tier I thresholds are transported via a one-shot quantile-alignment map fitted on baseline data. Threshold lines on all plots match the values used at runtime (from the code/audit logs).

A. Tier I: Adversarial Monte Carlo

Setup. Job sizes $n \in \{4, 8, 16\}$; workloads: **none** (baseline), **r1** (batch-size modulation), **timing** (periodic burst injection). Each run uses 40 seeds for 800 steps, producing per-interval leakage $\hat{\Delta}_t$, policy traces, and cost metrics. Thresholds $(\Delta_{\text{budget}}, \Delta_{\text{kill}})$ are chosen per experiment as above. The policy mechanics (strike/cooldown with $(\Delta_{\text{budget}}, \Delta_{\text{kill}})$) are specified in Sec. IV.

The leakage distributions in Fig. 3 show baseline mass concentrated below Δ_{budget} , with **r1** shifting $\hat{\Delta}_t$ moderately to the right and **timing** producing the heaviest right tails

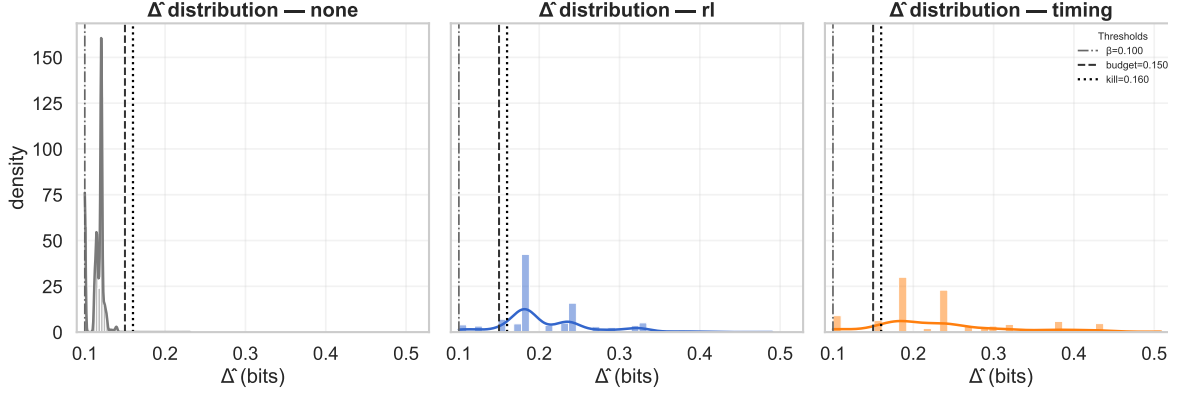


Fig. 3. **Tier I: leakage distributions.** Histograms of $\hat{\Delta}_t$ for baseline and adversarial workloads. Vertical lines denote the exact (Δ_{budget} , Δ_{kill}) used in this experiment (from the code logs). Baseline mass lies below Δ_{budget} ; *rl* shifts the distribution; *timing* induces heavier right tails, approaching/exceeding Δ_{kill} .

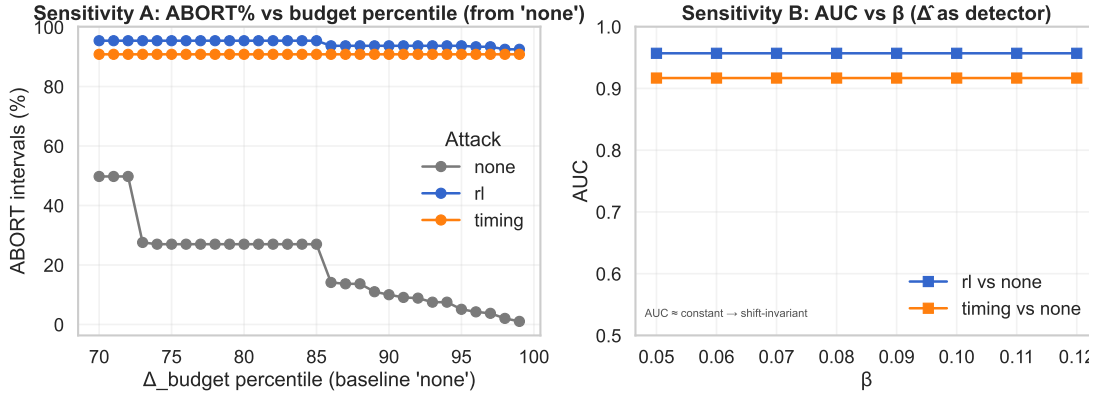


Fig. 4. **Tier I: threshold sensitivity.** Varying Δ_{budget} at a fixed hysteresis gap demonstrates robust detection across operating points: tighter budgets yield higher detection at the expense of higher abort rates, as expected.

that approach or exceed Δ_{kill} . Vertical lines mark the exact (Δ_{budget} , Δ_{kill}) emitted by the code/logs for each panel, making the operating point explicit relative to the induced tails.

Sweeping Δ_{budget} at a fixed hysteresis gap, as in Fig. 4, indicates robust detection across operating points: tightening the budget improves separability while increasing abort rates in a predictable manner, demonstrating that conclusions are not contingent on a single threshold pair.

Detailed latency and power impacts are deferred to Tier II, where costs are reported *per admitted interval*; benign overheads remain small, while adversarial pressure increases both latency and power with clear scaling in n .

B. Tier II: Cloud–Hardware Emulation

Setup. We emulate realistic backend heterogeneity, FIFO queues, dispatch jitter, and CASQUE routing without vendor APIs. Workloads use $n \in \{4, 8\}$ with the same seeds as Tier I. Calibration artefacts (q_{ref} , β) remain locked. Thresholds (Δ_{budget} , Δ_{kill}) are obtained per experiment via the quantile-alignment transfer from Tier I and are recorded in the

experimentation code/logs; plotted threshold lines match those artefacts.

Leakage distributions.: Per-interval histograms of $\hat{\Delta}_t$ show baseline mass concentrated below Δ_{budget} , a moderate right-shift for *rl*, and the heaviest right tails under *timing*, approaching or exceeding Δ_{kill} . Each panel annotates the exact per-experiment (Δ_{budget} , Δ_{kill}), making the operating point clear relative to induced tails (Fig. 5).

Policy outcomes and scaling.: Interval-level ABORT rates increase under adversarial workloads and scale with n , with *timing* producing the highest incidence. This pattern mirrors the heavier leakage tails and indicates that the policy enforces the intended WARN/ABORT behaviour as pressure grows (left panel in Fig. 6).

Cost trade-offs (per admitted interval).: Latency and power remain close to baseline under *none*, but both rise under adversarial pressure—strongest for *timing*—with growth in n consistent with queue stress and routing constraints. Reporting *per admitted interval* isolates performance impact from episode truncation (middle/right panels in Fig. 6).

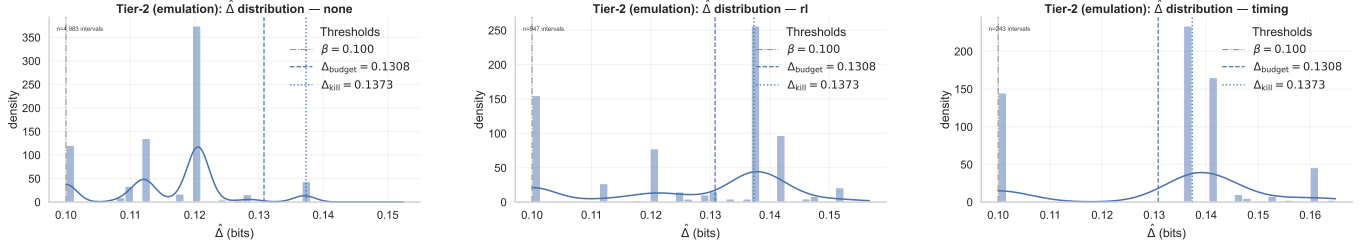


Fig. 5. **Tier II leakage histograms (per admitted interval).** *Left:* baseline (none) mass lies below Δ_{budget} . *Middle:* r1 shifts $\hat{\Delta}_t$ right. *Right:* timing induces heavier right tails that approach/exceed Δ_{kill} . Threshold lines are the exact per-experiment (Δ_{budget} , Δ_{kill}) emitted by the code/logs.

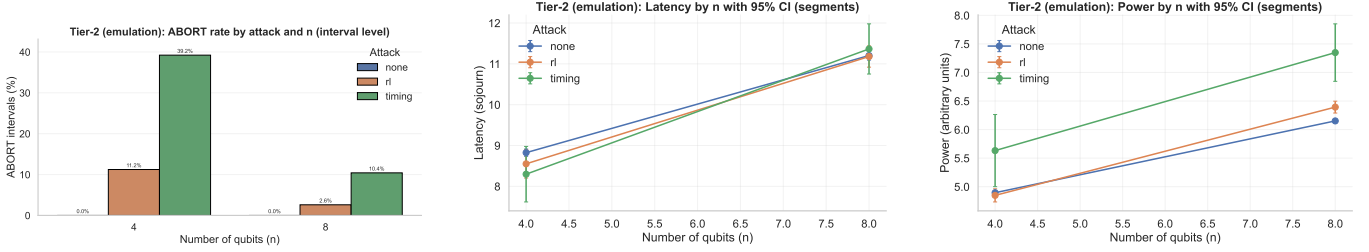


Fig. 6. **Tier II outcomes and costs (per admitted interval).** *Left:* ABORT rate by attack and $n \in \{4, 8\}$. *Middle:* latency vs. n with 95% CIs. *Right:* power vs. n with 95% CIs. Adversarial workloads (especially timing) raise ABORT incidence and increase latency/power, consistent with the heavier leakage tails in Fig. 5.

VII. DISCUSSION AND CONCLUSION

NADGO delivers *per-interval operational privacy* for gate-model quantum clouds by combining hardware-aware t -design padding, drift-robust timing randomisation, CASQUE topology-aware routing, and an online leakage estimator $\hat{\Delta}_t$ governed by locked thresholds (Δ_{budget} , Δ_{kill}) under the OP-IND framework (Sec. V). Across Tier I (Monte Carlo) and Tier II (queue/timing-aware emulation), baseline operation concentrates mass below budget with low abort incidence, while adversarial workloads shift leakage toward policy boundaries and elicit policy-compliant WARN/ABORT outcomes, with performance costs measured *per admitted interval* remaining modest under benign load and rising under attack with clear scaling in n . The calibration artefacts are locked across tiers and thresholds are recorded per experiment for auditability. Limitations include abstraction of proprietary vendor behaviours and evaluation on small tiles; future work will address scaling, adaptive/coordinated adversaries, multi-region routing with topology-specific budgets, and succinct proofs of interval-level policy enforcement. Overall, by unifying leakage-aware compilation, drift-adaptive scheduling, and auditable enforcement, NADGO provides a practical path to certifiable operational privacy at low overhead in multi-tenant quantum clouds.

REFERENCES

- [1] J. F. Fitzsimons, “Private quantum computation: An introduction to blind quantum computing and related protocols,” *npj Quantum Information*, vol. 3, no. 1, p. 23, 2017. DOI: 10.1038/s41534-017-0025-3. [Online]. Available: <https://doi.org/10.1038/s41534-017-0025-3>.
- [2] C. Lu, E. Telang, A. Aysu, and K. Basu, *Quantum leak: Timing side-channel attacks on cloud-based quantum services*, 2024. arXiv: 2401.01521 [cs.ET]. [Online]. Available: <https://arxiv.org/abs/2401.01521>.
- [3] Y. Mustafa and S. Köse, “Side-channel leakage in sfq circuits and related attacks on qubit control and readout systems,” *IEEE Transactions on Applied Superconductivity*, vol. 33, no. 6, pp. 1–7, 2023. DOI: 10.1109/TASC.2023.3277864. [Online]. Available: <https://doi.org/10.1109/TASC.2023.3277864>.
- [4] A. Ambainis and J. Emerson, *Quantum t -designs: t -wise independence in the quantum world*, 2007. arXiv: quant-ph/0701126 [quant-ph]. [Online]. Available: <https://arxiv.org/abs/quant-ph/0701126>.
- [5] F. G. S. L. Brandão, A. W. Harrow, and M. Horodecki, “Local random quantum circuits are approximate polynomial-designs,” *Communications in Mathematical Physics*, vol. 346, no. 2, pp. 397–434, Aug. 2016. DOI: 10.1007/s00220-016-2706-8. [Online]. Available: <https://doi.org/10.1007/s00220-016-2706-8>.
- [6] J. Haferkamp, “Random quantum circuits are approximate unitary t -designs in depth $O(nt^{5+o(1)})$,” *Quantum*, vol. 6, p. 795, 2022. DOI: 10.22331/q-2022-09-08-795. arXiv: 2203.16571 [quant-ph]. [Online]. Available: <https://doi.org/10.22331/q-2022-09-08-795>.
- [7] H. Kurniawan, L. Rodríguez-Soriano, D. Cuomo, C. G. Almudéver, and F. G. Herrero, “On the use of calibration data in error-aware compilation techniques for nisq devices,” in *2024 IEEE International Conference on Quantum Computing and Engineering (QCE)*, vol. 01,

2024, pp. 338–348. doi: 10.1109/QCE60285.2024.00048. [Online]. Available: <https://doi.org/10.1109/QCE60285.2024.00048>.

- [8] D. Ferrari and M. Amoretti, “Noise-adaptive quantum compilation strategies evaluated with application-motivated benchmarks,” *arXiv preprint arXiv:2108.11874*, 2021. doi: 10.48550/arXiv.2108.11874. arXiv: 2108 . 11874 [quant-ph]. [Online]. Available: <https://doi.org/10.48550/arXiv.2108.11874>.
- [9] J. Mardia, J. Jiao, E. Tánzos, R. D. Nowak, and T. Weissman, *Concentration inequalities for the empirical distribution*, 2019. arXiv: 1809.06522 [cs.IT]. [Online]. Available: <https://arxiv.org/abs/1809.06522>.
- [10] H. Wang *et al.*, “Quantumnas: Noise-adaptive search for robust quantum circuits,” in *2022 IEEE International Symposium on High-Performance Computer Architecture (HPCA)*, IEEE, Apr. 2022, pp. 692–708. doi: 10.1109/HPCA53966.2022.00057. [Online]. Available: <https://doi.org/10.1109/HPCA53966.2022.00057>.
- [11] J. Pérez-Bailón, M. Tarancón, S. Celma, and C. Sánchez-Azqueta, “Cryogenic measurement of cmos devices for quantum technologies,” *IEEE Transactions on Instrumentation and Measurement*, vol. 72, pp. 1–7, 2023. doi: 10.1109/TIM.2023.3325446. [Online]. Available: <https://doi.org/10.1109/TIM.2023.3325446>.
- [12] J. Eastoe, G. M. Noah, D. Dutta, A. Rossi, J. D. Fletcher, and A. Gomez-Saiz, “Method for efficient large-scale cryogenic characterization of cmos technologies,” *IEEE Transactions on Instrumentation and Measurement*, vol. 74, pp. 1–10, 2025.
- [13] A. Rehman, V. Langford, J. John, and Y. Liu, “Opaque: Obfuscating phase in quantum circuit compilation for efficient ip protection,” in *2025 26th International Symposium on Quality Electronic Design (ISQED)*, 2025, pp. 1–6. doi: 10 . 1109 / ISQED65160 . 2025 . 11014313. [Online]. Available: <https://doi.org/10.1109/ISQED65160.2025.11014313>.